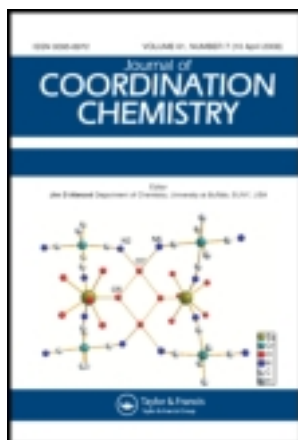


This article was downloaded by: [Renmin University of China]

On: 13 October 2013, At: 10:25

Publisher: Taylor & Francis

Informa Ltd Registered in England and Wales Registered Number: 1072954 Registered office: Mortimer House, 37-41 Mortimer Street, London W1T 3JH, UK



## Journal of Coordination Chemistry

Publication details, including instructions for authors and subscription information:

<http://www.tandfonline.com/loi/gcoo20>

### Spectroscopic investigations of hematoxylin-Eu(III) complex interacting with Herring-sperm DNA

Jianhang Huang <sup>a</sup>, Xingming Wang <sup>a</sup> & Lisheng Ding <sup>b</sup>

<sup>a</sup> School of Materials Science and Engineering, Southwest University of Science and Technology, Mianyang 621010, China

<sup>b</sup> Chengdu Institute of Biology, Chinese Academy of Sciences, Chengdu 610041, China

Published online: 09 Aug 2011.

To cite this article: Jianhang Huang, Xingming Wang & Lisheng Ding (2011) Spectroscopic investigations of hematoxylin-Eu(III) complex interacting with Herring-sperm DNA, *Journal of Coordination Chemistry*, 64:16, 2791-2803, DOI: [10.1080/00958972.2011.607234](https://doi.org/10.1080/00958972.2011.607234)

To link to this article: <http://dx.doi.org/10.1080/00958972.2011.607234>

PLEASE SCROLL DOWN FOR ARTICLE

Taylor & Francis makes every effort to ensure the accuracy of all the information (the "Content") contained in the publications on our platform. However, Taylor & Francis, our agents, and our licensors make no representations or warranties whatsoever as to the accuracy, completeness, or suitability for any purpose of the Content. Any opinions and views expressed in this publication are the opinions and views of the authors, and are not the views of or endorsed by Taylor & Francis. The accuracy of the Content should not be relied upon and should be independently verified with primary sources of information. Taylor and Francis shall not be liable for any losses, actions, claims, proceedings, demands, costs, expenses, damages, and other liabilities whatsoever or howsoever caused arising directly or indirectly in connection with, in relation to or arising out of the use of the Content.

This article may be used for research, teaching, and private study purposes. Any substantial or systematic reproduction, redistribution, reselling, loan, sub-licensing, systematic supply, or distribution in any form to anyone is expressly forbidden. Terms & Conditions of access and use can be found at <http://www.tandfonline.com/page/terms-and-conditions>

## Spectroscopic investigations of hematoxylin–Eu(III) complex interacting with Herring-sperm DNA

JIANHANG HUANG<sup>†</sup>, XINGMING WANG<sup>\*†</sup> and LISHENG DING<sup>‡</sup>

<sup>†</sup>School of Materials Science and Engineering, Southwest University of Science and Technology, Mianyang 621010, China

<sup>‡</sup>Chengdu Institute of Biology, Chinese Academy of Sciences, Chengdu 610041, China

(Received 24 September 2010; in final form 6 July 2011)

The interaction of HE–Eu(III) complex (HE=hematoxylin) with Herring-sperm DNA (hsDNA) has been studied by absorption spectra, fluorescence, and viscosity measurements in physiological buffer (pH = 7.40). The binding constant of HE–Eu(III) complex to hsDNA was obtained by double reciprocal method at 298 and 310 K and the corresponding thermodynamic parameters ( $\Delta_r H_m^\ominus = 8.55 \times 10^4 \text{ J mol}^{-1}$ ,  $\Delta_r G_m^\ominus = -3.01 \times 10^4 \text{ J mol}^{-1}$ ,  $\Delta_r S_m^\ominus = 387.95 \text{ J mol}^{-1} \text{ K}^{-1}$ ) were calculated, showing that the interaction between HE–Eu(III) complex and hsDNA was driven mainly by entropy. The value of  $K$  indicated that the binding mode of HE–Eu(III) complex with DNA was not classical intercalation. These results were further supported by viscosity method and competitive binding experiment. Scatchard analysis suggests that the interaction mode was a mixed binding, which contains partial intercalation and groove binding.

*Keywords:* Spectroscopy; Hematoxylin; Eu(III); Herring-sperm DNA; Interaction

### 1. Introduction

Numerous experiments have demonstrated that DNA is the primary intracellular target of anticancer drugs due to the interaction between small molecules and DNA, which damages cancer cell's DNA, blocking the division of cancer cells and resulting in cell death. The interaction of DNA with other molecules is an important fundamental issue for life sciences [1–5]. Rare earth metals have strong affinity with cancer cell and can interfere with the metabolism of cancer cells. Bio-pharmacological functions of rare earth complexes have been extensively studied, which gave valuable information about DNA structural properties, gene mutation, nature of different diseases, action mechanisms of some antitumor drugs, new probes, and labels for analysis of nucleic acids [6–8].

Flavonoids have a variety of biological effects in mammalian cell systems and have been reported to have important medical functions such as antiviral, anti-allergic, anti-platelet, anti-inflammatory, and anti-tumor activities, and possibly even protective effects against chronic diseases [2]. Hematoxylin is a derivative of catechol, which is one

\*Corresponding author. Email: xmwang\_xkd@yahoo.cn

of the most bioactive flavonoids [9]. Studies in the past few years indicate that hematoxylin has remarkable inhibitory action to stomach cancer [10, 11]. The interaction of rare earth metal complexes with DNA has attracted attention, because rare earth metals have more physiological activities and lower toxicities after coordination [7]. In this article, we synthesize and characterize the HE–Eu(III) complex. DNA binding of the complex was investigated by electronic absorption spectroscopy, fluorescence spectroscopy, and viscosity measurements. Experimental evidence indicates that the complex can strongly bind to Herring-sperm DNA (hsDNA) through partial intercalation and groove binding mode. Information obtained from these studies provides insight into the mechanism of interactions of rare earth complexes with DNA and will also be helpful in developing new antioxidants.

## 2. Materials and methods

### 2.1. Materials

hsDNA was purchased from Sigma Biological Co. and used as received. All samples were dissolved in Tris-HCl buffer. HE (figure 1) was purchased from Sichuan Chengdu China Kelong chemical plant (A.R.).  $\text{Eu}_2\text{O}_3$  was purchased from Beifang Fangzheng rare metal lab company (99.99%) and dissolved in dense HCl, then HCl was vaporized slowly to get  $\text{EuCl}_3$  solution in different concentrations. Acridine orange (AO) was purchased from Shanghai-China medicine chemical plant (A.R.). Other reagents were at least of analytical grade and used without purification.

### 2.2. Instruments

Absorption spectra were recorded on a UV-3150 spectrophotometer made by Japan Shimadzu. Fluorescence spectra were recorded on a FL-4500 spectrofluorophotometer made by Japan Hitachi. Infrared spectra were recorded on a Spectrum One spectrometer made by PE Instrument Co. USA. X-ray diffraction was conducted on an X'Pert PRO diffractometer made by PAN-alytical B.V. at a voltage of 45 kV and a current of 50 mA. The sample was analyzed in the  $2\theta$  angle range  $3\text{--}90^\circ$  and the process parameters were set as: scan step size of  $0.02^\circ$ , scan step time of 1.54 s. HPLC/MS was conducted on a Varian 1200LC/MC. The pH was recorded on a pHs-2C acidometer (made in China). In fluorescence mode, both excitation and emission bandwidths were

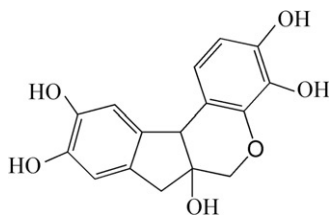


Figure 1. Structure of hematoxylin.

set at 5 nm,  $\lambda_{\text{ex}} = 441$  nm. All spectroscopic work was carried out at pH 7.40 maintained by a Tris-HCl buffer.

### 2.3. Preparation of the complex

The complex was prepared by adding stoichiometric europium chloride solution into HE solution dropwise; the resulting solution was refluxed for 6 h at 353 K. Kept stationary at room temperature, aubergine crystals were obtained, washed with ethanol, and dried in a desiccator. Infrared spectra of free hematoxylin in KBr pellets showed stretching vibration band at  $1234\text{ cm}^{-1}$  ( $\nu_{\text{CO}}$ ). Upon binding to Eu(III), the complex exhibits a band at  $1207\text{ cm}^{-1}$  ( $\nu_{\text{CO}}$ ), which indicates the coordination of Eu(III) to the oxygen of hydroxy. This was supported by the appearance of a new medium intensity band at  $470\text{--}500\text{ cm}^{-1}$  assigned to (M–O) vibration. Elemental analysis: observed C 45.14, H 3.69; calcd C 46.52, H 3.63 for  $[\text{Eu}(\text{HE})_2 \cdot 2\text{H}_2\text{O} \cdot \text{Cl}]$ . The complex belongs to the monoclinic crystal system, unit cell parameters are  $a = 14.443\text{ \AA}$ ,  $b = 24.575\text{ \AA}$ ,  $c = 19.077\text{ \AA}$ ,  $\alpha = 90^\circ$ ,  $\beta = 98.23^\circ$ ,  $\gamma = 90^\circ$ , and the complex is shown in figure 2. The mass spectrum of HE–Eu(III) complex shows peaks at  $m/z$  of 773 and 791, which can be assigned to fragments  $[\text{Eu}(\text{HE})_2 \cdot \text{H}_2\text{O}]^+$  and  $[\text{Eu}(\text{HE})_2 \cdot 2\text{H}_2\text{O}]^+$ , respectively.

### 2.4. Spectral measurements

Spectral measurements were performed by the spectrophotometric titration method. Each injection is  $10\text{ }\mu\text{L}$  so the volume change was so small that could be ignored; Tris-HCl buffer solution worked as the reference solution. All solutions were shaken thoroughly and allowed to equilibrate for 10 min before spectral measurements were made at room temperature.

Scatchard method was conducted as follows: DNA was incubated with different  $R_t$  ( $R_t = [\text{HE–Eu(III) complex}]/[\text{DNA}]$ ,  $R_t = 0.00, 0.50, 1.00, \text{ and } 1.50$ , respectively) of HE–Eu(III) complex for 10 min, then the samples were titrated by AO solution and the fluorescence intensity was measured.

Hydroxyl radical scavenging activity of HE–Eu(III) was performed by the literature method [12], with some modifications. The reaction mixture of 10 mL contained  $0.5\text{ mL}$  of  $9\text{ mmol L}^{-1}$   $\text{FeSO}_4$ ,  $2\text{ mL}$  HE–Eu(III) complex solution,  $0.5\text{ mL}$  of  $9\text{ mmol L}^{-1}$  salicylic acid alcohol solution,  $6.5\text{ mL}$  distilled water, and  $0.5\text{ mL}$  of  $8.8\text{ mmol L}^{-1}$  hydrogen peroxide; after incubation for 1 h at  $37^\circ\text{C}$ , the absorbance of reaction system ( $A_1$ ) was measured at 510 nm. The scavenging activity of hydroxyl radical was

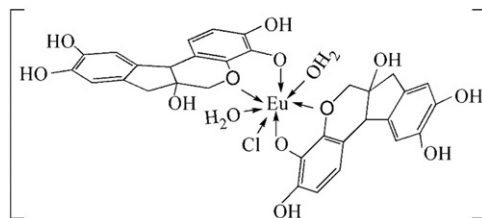


Figure 2. The possible structure of the HE–Eu(III) complex.

calculated as follows:  $[1 - (A_1 - A_2)/A_0] \times 100\%$ , where  $A_0$  is the absorbance of the control (distilled water instead of the complex) and  $A_2$  is the absorbance of the control (distilled water instead of  $\text{FeSO}_4$ ).

## 2.5. Viscosity measurements

Viscosity measurements were performed using a viscometer, which was immersed in a thermostated water-bath at room temperature. Different amounts of HE–Eu complex were added into the viscometer, while keeping the DNA concentration constant. The flow times were above 200 s, and each point measured was the average of at least three readings. The data were presented as  $\eta/\eta_0$  versus [HE–Eu(III) complex], where  $\eta$  and  $\eta_0$  are the viscosity of DNA in the presence and absence of the complex, respectively.

## 3. Results and discussion

### 3.1. Absorption spectra of interaction between HE and Eu(III)

The complexes show absorbance due to metal-to-ligand charge transfer. Absorption spectra of HE at physiological pH in the absence and presence of different amounts of Eu(III) are shown in figure 3; when Eu(III) was added to a solution of HE, one broad peak at 600 nm appeared while the intensity of the ligand peak at 208 nm decreased; there was one isosbestic point at 225 nm. These phenomena were indicative of the interaction between Eu(III) and HE [13]. HE exhibited an absorption at 289 nm, attributed to the  $n-\pi^*$  of the heteroatom oxygen, the absorption increased and blue shifted to 288 nm with the addition of Eu(III), implying that coordination takes place between Eu(III) and oxygen. In order to determine the stoichiometry of the europium complex in solution, a mole-ratio study was performed at 600 nm. In the mole-ratio

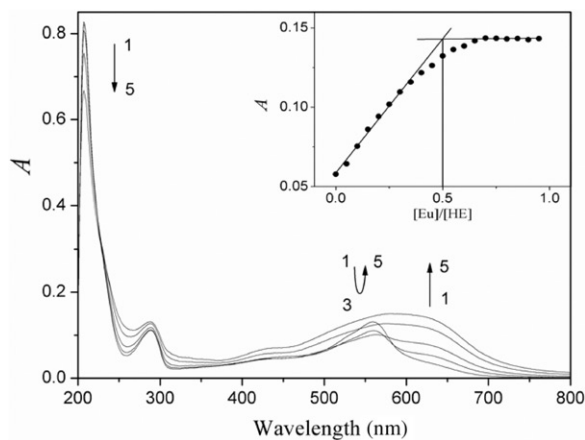


Figure 3. Absorption spectra of HE in different concentrations of Eu(III);  $[\text{HE}] = 2.00 \times 10^{-5} \text{ mol L}^{-1}$ ,  $[\text{Eu}] = 3.00 \times 10^{-4} \text{ mol L}^{-1}$  (10  $\mu\text{L}$  per scan). Inset: mole-ratio plots of HE–Eu(III).

plots, two lines were obtained (inset in figure 3); the intersection suggested that the stoichiometry of the complex in solution for metal to ligand was 1 : 2.

### 3.2. Spectroscopic study of the interaction between HE–Eu(III) complex and DNA

Electronic absorption spectroscopy is one of the most useful techniques to investigate the interaction of complexes with DNA. The absorption intensity of the complexes was observed from 200 to 800 nm (figure 4). With increasing concentration of hsDNA solution, the intensity of the metal-to-ligand charge transfer band (at 600 nm) started increasing. In general, hypochromism and red shift are associated with the classical intercalative binding of the complex to the helix, due to strong stacking interactions between the aromatic chromophore of the complex and the base pairs of DNA [14], but it was not observed in the absorption spectra, indicating that the binding mode of HE–Eu(III) complex with DNA was not classical intercalation. Upon addition of hsDNA, absorption bands at 209 and 600 nm showed hyperchromism, accompanied by red shift at 209 nm (from 209 to 213 nm). These results may be due to the dissociation of ligand aggregates or external contact (surface binding) with the double helix, the small change in  $\lambda_{\max}$  was more in keeping with groove binding, leading to small perturbations [15, 16]. Deprotonation on phenol of HE was favorable in solution, and negative ion of phenol could interact with the major or minor grooves of hsDNA through hydrogen bonds, and the  $\pi$ – $\pi^*$  orbital of the bound ligand could couple with the  $\pi$  orbital of the base pairs, decreasing  $\pi$ – $\pi^*$  transition energy, which results in bathochromic shift. From the mole-ratio plots (inset in figure 4), the stoichiometry of the complex in solution for DNA to HE–Eu(III) complex was about 1 : 5.

Fluorescence spectra of HE–Eu(III) complex (figure 5) increase in intensity when the DNA solution is added, implying that HE–Eu(III) complex binds to DNA. It may be due to the increase in the molecular planarity of the complex and decrease in the collision frequency of solvent with the complex, caused by the planar aromatic group of the complex stacking between adjacent base pairs of DNA [7].

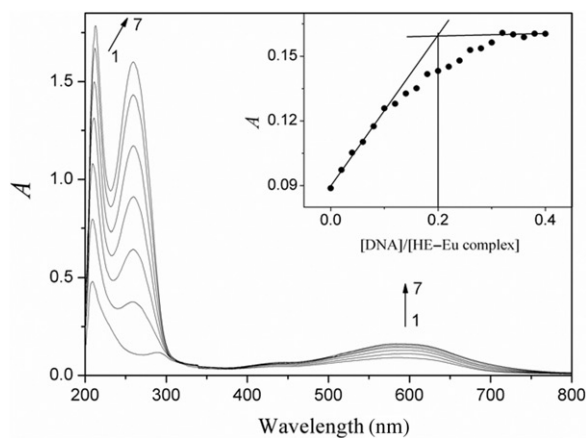


Figure 4. Absorption spectra of HE–Eu(III) complex in different concentrations of DNA; [HE–Eu(III) complex] =  $1.00 \times 10^{-5} \text{ mol L}^{-1}$ , [DNA] =  $6.00 \times 10^{-5} \text{ mol L}^{-1}$  (10  $\mu\text{L}$  per scan). Inset: mole-ratio plots of HE–Eu(III)–DNA.

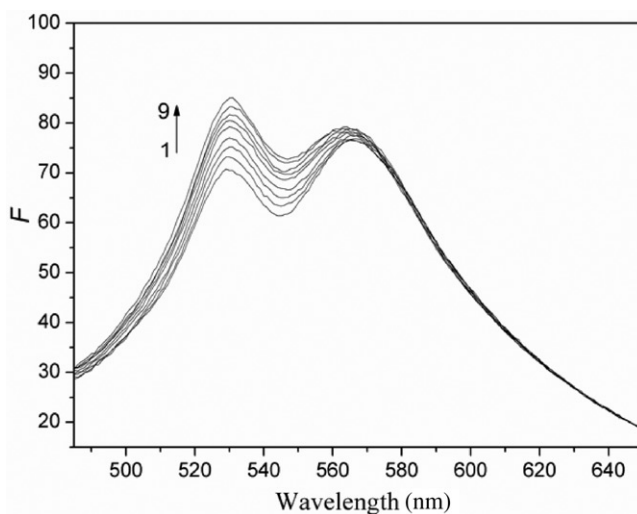


Figure 5. Emission spectra of HE–Eu(III) complex in different concentrations of DNA; [HE–Eu(III) complex] =  $1.00 \times 10^{-5} \text{ mol L}^{-1}$ , [DNA] =  $6.00 \times 10^{-5} \text{ mol L}^{-1}$  (10  $\mu\text{L}$  per scan).

### 3.3. Double reciprocal method and thermodynamics studies

The intrinsic binding constant  $K$  was determined to estimate the magnitude of the binding strength of HE–Eu(III) complex with DNA. The intrinsic binding constant can be obtained by monitoring the changes in the absorbance at  $\lambda_{\text{max}} = 600 \text{ nm}$  with increasing concentrations of DNA, given by the ratio of the slope to the  $y$  intercept in plots  $1/(A_0 - A)$  versus  $1/[\text{DNA}]$  (figure 6), according to the following equation [17, 18]:

$$1/(A_0 - A) = 1/A_0 + 1/(K \times A_0 \times [\text{DNA}]),$$

where  $A_0$  is the absorbance of HE–Eu(III) complex in the absence of DNA,  $A$  is the absorbance of HE–Eu(III) complex in the presence of DNA,  $K$  is the binding constant between HE–Eu(III) complex and hsDNA, and [DNA] is the concentration of DNA. According to the above equation,  $K$  values at two temperatures (298 and 310 K):  $K_{298\text{K}}^{\ominus} = 1.90 \times 10^5 \text{ L mol}^{-1}$ ,  $K_{310\text{K}}^{\ominus} = 7.21 \times 10^5 \text{ L mol}^{-1}$  are obtained.  $K$  values are lower than those observed for classical intercalators, indicating that DNA bonding has an affinity less than classical intercalators [19].

Thermodynamic parameters dependent on temperatures were analyzed to further characterize the interaction between HE–Eu(III) complex and DNA. If the enthalpy change ( $\Delta_r H m^{\ominus}$ ) does not vary significantly over the temperature range studied, then its value and that of entropy change ( $\Delta_r S m^{\ominus}$ ) can be determined from the van't Hoff equation:

$$\log K^{\ominus} = -\Delta_r H m^{\ominus}/(2.303RT) + \Delta_r S m^{\ominus}/(2.303R),$$

where  $K$  and  $R$  are the binding and gas constants, respectively. Then,  $\Delta_r H m^{\ominus} = 8.55 \times 10^4 \text{ J mol}^{-1}$  and  $\Delta_r S m^{\ominus} = 387.95 \text{ J mol}^{-1}$  were deduced. The free energy change ( $\Delta_r G m^{\ominus}$ ) of  $-3.01 \times 10^4 \text{ J mol}^{-1}$  at 298 K was deduced.

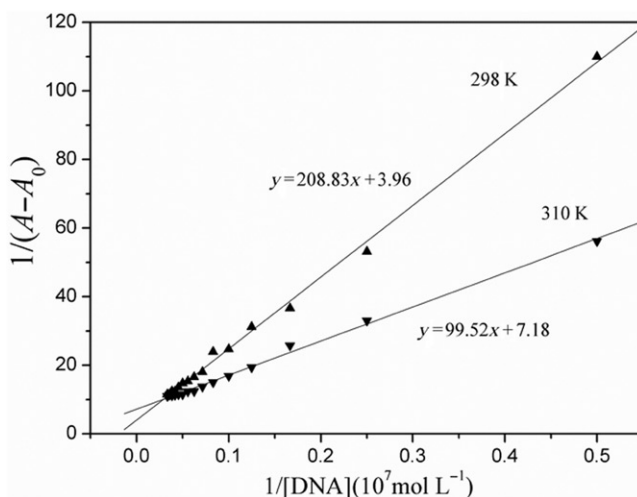


Figure 6. Double reciprocal plots of HE–Fe(III)–DNA; [HE–Eu(III) complex] =  $1.00 \times 10^{-5}$  mol L $^{-1}$ .

The negative value  $\Delta_r G_m^\ominus$  revealed that the interaction was spontaneous, both positive  $\Delta_r H_m^\ominus$  and  $\Delta_r S_m^\ominus$  values indicated that the entropy was favorable for the interaction of HE–Eu(III) complex with DNA, namely the process was driven mainly by entropy.

### 3.4. Competitive binding experiments using AO as probe

Although DNA has natural fluorescence, the intensity is so weak that the direct use of the fluorescence emission of DNA is limited. AO was selected as a fluorescence probe because of its known spectral and self-aggregation characteristics, and it is widely used as a fluorescence chromophore marker for DNA; AO's fluorescence is strongly enhanced when intercalated into DNA base pairs [20]. If HE–Eu(III) complex and AO have the same binding mode with hsDNA, HE–Eu(III) complex could compete with AO for intercalation into hsDNA, and the fluorescence could be quenched by the addition of HE–Eu(III). Emission intensities of DNA–AO system were measured (figure 7). There are two quenching processes, static and dynamic. Fluorescence quenching can be dynamic, resulting from the collisional encounters between the fluorophore and quencher, or static, resulting from the formation of a ground-state complex between the fluorophore and quencher [21]. The Stern–Volmer constant  $K_{SV}$  is often used to evaluate the quenching efficiency for a compound; it is given by the equation [22]:

$$F_0/F = 1 + K_{SV}[\text{complex}] = 1 + K_q \tau_0[\text{complex}],$$

where  $F_0$  and  $F$  are the emission intensities in the absence and the presence of the complex, respectively,  $K_q$  is the DNA–AO quenching rate constant,  $\tau_0$  is the average lifetime of DNA–AO in the absence of the complex and its value is  $10^{-9}$  to  $10^{-7}$  s [22],  $[\text{complex}]$  is the complex concentration, and  $K_{SV}$  is the quenching constant and equals



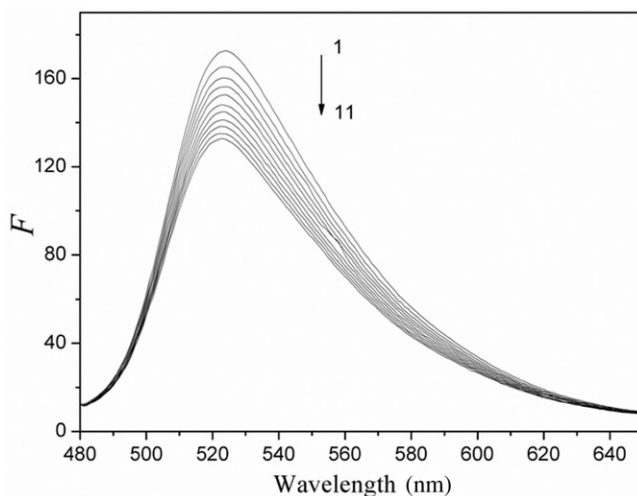


Figure 7. Emission spectra of DNA-AO admixture in different concentrations of HE-Eu(III) complex;  $[\text{DNA-AO}] = 1.00 \times 10^{-7} \text{ mol L}^{-1}$ ;  $[\text{HE-Eu(III) complex}] = 1.00 \times 10^{-5} \text{ mol L}^{-1}$  (10  $\mu\text{L}$  per scan).

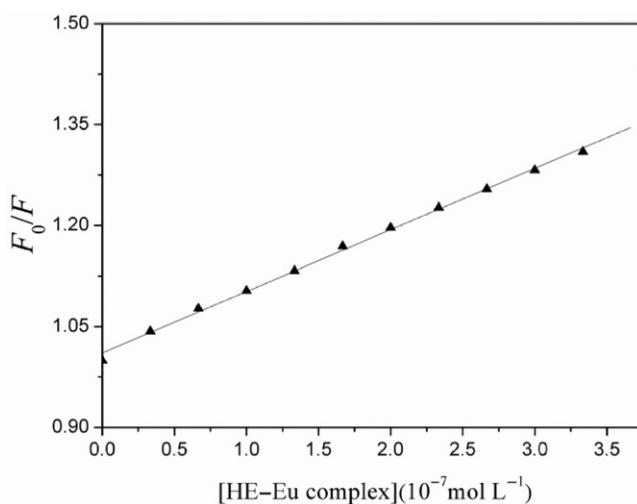


Figure 8. The Stern-Volmer plots for the quenching of DNA-AO by HE-Eu(III) complex.

$K_q$  multiplied by  $\tau_0$ . Both static and dynamic quenching are in agreement with a linear Stern-Volmer equation. Based on the Stern-Volmer equation (figure 8),  $K_q$  can be obtained:  $K_q = 9.13 \times 10^{12-14} \text{ L s}^{-1} \text{ mol}^{-1}$ . For the HE-Eu(III) complex, the values of  $K_q$  are much greater than  $2.0 \times 10^{10} \text{ L s}^{-1} \text{ mol}^{-1}$ , the maximum diffusion collision quenching rate constant of various quenchers with biopolymers [23]. The experimental results demonstrate that the quenching process was static quenching; HE-Eu(III) complex can compete with AO for intercalation into hsDNA.

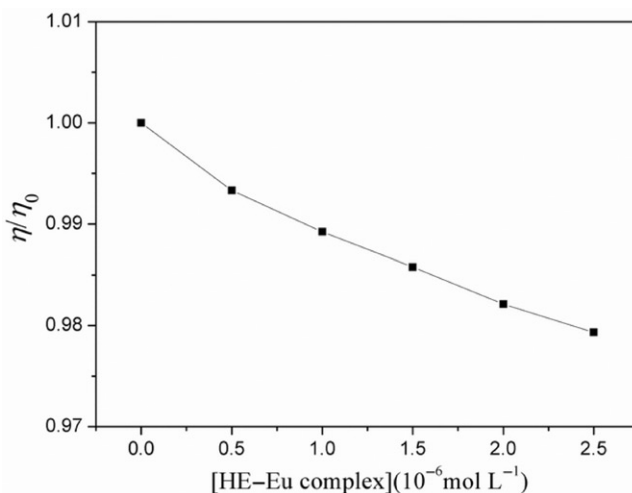


Figure 9. Influence on DNA viscosity with different concentrations of HE–Eu(III) complex. [DNA] =  $1.00 \times 10^{-5} \text{ mol L}^{-1}$ .

### 3.5. Viscosity method

Hydrodynamic measurement such as viscosity is the least ambiguous and the most critical test of binding mode in solution in the absence of crystallographic structural data. A classical intercalation model often causes lengthening of the DNA helix, while in the groove binding or electrostatic mode, the length of the helix is unchanged with no apparent alteration in DNA viscosity. Partial and non-classical intercalation could bend (or kink) the DNA helix, thereby reducing its viscosity [24]. As illustrated in figure 9, as the amounts of HE–Eu(III) complex increased, the viscosity of DNA decreased steadily, suggesting that the complex is partially inserted into the DNA base pairs resulting in a bend or kink in the DNA helix. Combined with the above result and competitive binding experiments, there exists partial intercalation binding between HE–Eu(III) complex and DNA.

### 3.6. Scatchard analysis

In order to further understand the mechanisms of DNA–drug interaction, we conducted a Scatchard analysis. The characteristics of binding of AO to DNA can be expressed by the Scatchard equation [25, 26]:

$$r_{\text{AO}}/[\text{AO}] = K(n - r_{\text{AO}}),$$

where  $r_{\text{AO}}$  is the proportion of bound AO per nucleic acid phosphate, [AO] is the concentration of free AO,  $n$  is the number of binding sites per nucleic acid phosphate, and  $K$  is the intrinsic association constant to a site.

The Scatchard plots were obtained by using  $r_{\text{AO}}/[\text{AO}]$  as a function of  $r_{\text{AO}}$  (figure 10). It indicates an intercalation binding mode if the values of  $n$  were equal at different  $R_t$ , but not intercalation if the values of  $K$  were equal. A mixture of binding mode is

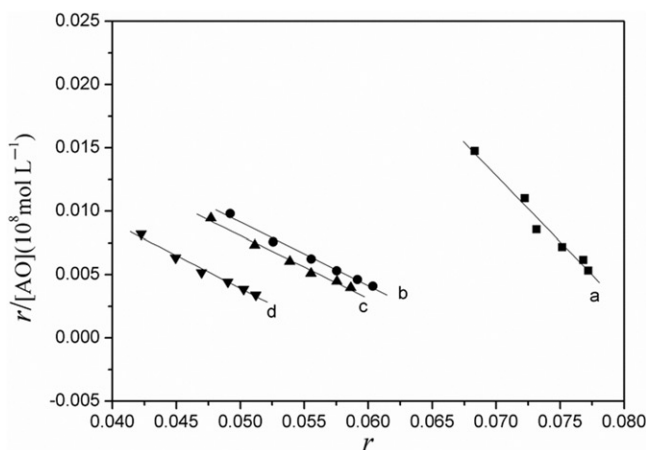


Figure 10. Scatchard plots of HE-Eu(III)-DNA in different concentrations of AO. [DNA] =  $2.00 \times 10^{-7} \text{ mol L}^{-1}$ ; [AO] =  $6.00 \times 10^{-6} \text{ mol L}^{-1}$  (10  $\mu\text{L}$  per scan);  $R_t = [\text{HE-Eu(III) complex}]/[\text{DNA}]$ ; (a)  $R_t = 0.00$ ; (b)  $R_t = 0.50$ ; (c)  $R_t = 1.00$ ; (d)  $R_t = 1.50$ .

Table 1. Data of Scatchard equation of the interaction between HE-Eu(III) complex and DNA.

Curve	$c_{\text{HE-Eu(III) complex}}/c_{\text{DNA}}$	Scatchard equation	$K \text{ (L mol}^{-1}\text{)}$	$n$
a	0.00	$8.59 \times 10^6 - 1.04 \times 10^8 x$	$5.99 \times 10^7$	0.083
b	0.50	$3.43 \times 10^6 - 5.03 \times 10^7 x$	$3.37 \times 10^7$	0.068
c	1.00	$3.29 \times 10^6 - 4.96 \times 10^7 x$	$3.25 \times 10^7$	0.066
d	1.50	$2.98 \times 10^6 - 5.18 \times 10^7 x$	$3.69 \times 10^7$	0.058

indicated if both the values of  $n$  and  $K$  were changed [26, 27]. According to the Scatchard equation, the values of  $n$  and  $K$  are listed in table 1. Comparing the Scatchard plot of  $R_t = 0.00$  with  $R_t = 0.50$ , we found that both  $K$  and  $n$  values have changed, showing that the binding of complex and AO on DNA were not exactly the same and a mixed interaction at  $R_t = 0.50$ . Upon increasing the value of  $R_t$ , the  $n$  value in the Scatchard plot decreases but the  $K$  value remains almost unchanged, suggesting that at high values of  $R_t$ , HE-Eu(III) complex groove binds to DNA.

### 3.7. The influence of basic group to the HE-Eu(III) complex system

In order to further confirm the interaction between HE-Eu(III) complex and DNA, we studied the influence of the basic group to the complex system. There are two possibilities if the absorption spectrum of complex changes by adding base: first, HE-Eu(III) complex could affect the base pair of DNA through the major or minor groove of DNA, because in the major and minor grooves, bases are exposed to solvent and the complex can interact with the basic group directly. Second, complex can have a  $\pi-\pi$  interaction and hydrophobic interaction with the  $\pi$  system of base pair, which means intercalation. Figure 11 shows the influence of bases to the complex system; the

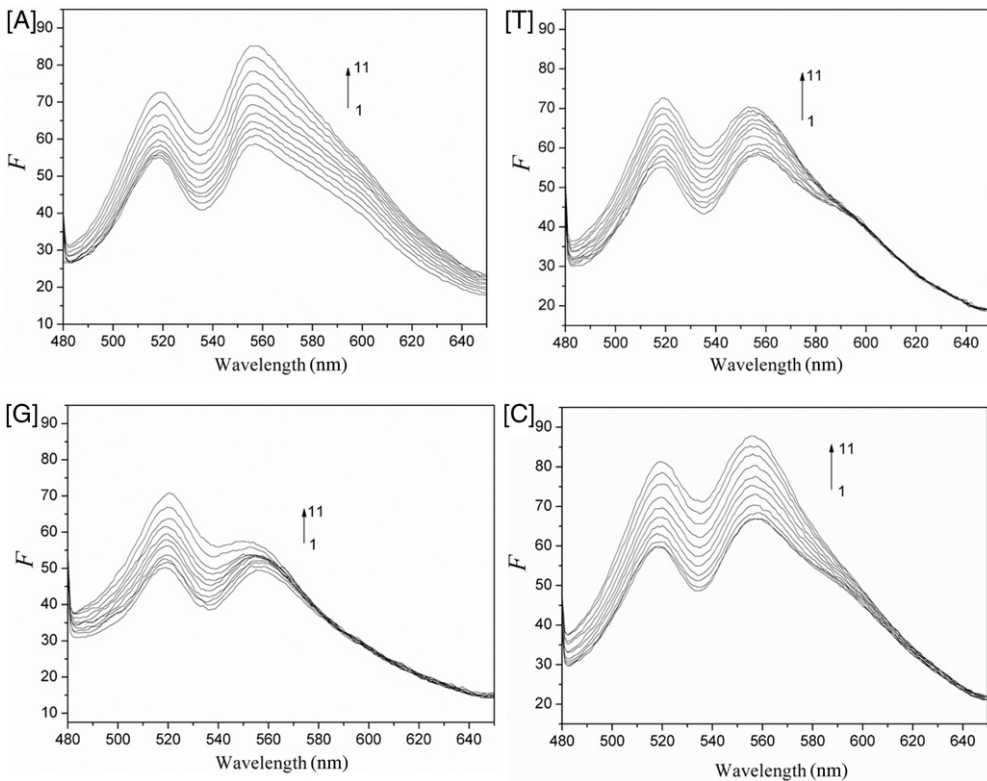


Figure 11. Emission spectra of HE–Eu(III) complex in different concentrations of the basic group [HE–Eu(III) complex] =  $1.00 \times 10^{-5} \text{ mol L}^{-1}$ ; [A] =  $5.00 \times 10^{-3} \text{ mol L}^{-1}$  (10  $\mu\text{L}$  per scan); [T] =  $5.00 \times 10^{-3} \text{ mol L}^{-1}$  (10  $\mu\text{L}$  per scan); [G] =  $5.00 \times 10^{-3} \text{ mol L}^{-1}$  (10  $\mu\text{L}$  per scan); and [C] =  $5.00 \times 10^{-3} \text{ mol L}^{-1}$  (10  $\mu\text{L}$  per scan).

emission spectrum of complex increased steadily with increasing amounts of A, T, C, and G, respectively, suggesting no selectivity in the interaction. Combined with the competitive binding study and the Scatchard method, the results identify that the interaction between HE–Eu(III) complex and DNA is partially intercalation binding and groove binding.

### 3.8. Studies on hydroxyl radical scavenging ability

$\cdot\text{OH}$  was generated by Fenton's reaction and trapped with salicylic acid. The  $\cdot\text{OH}$  scavenging activity of HE–Eu(III) complex was assessed by its ability to compete with salicylic acid for  $\cdot\text{OH}$  radicals. In this study, the hydroxyl radical-scavenging effect of the HE–Eu(III) complex (figure 12), in a concentration of  $6.0 \times 10^{-5} \text{ mol L}^{-1}$  was found to be 45.8% and in a concentration of  $8.0 \times 10^{-5} \text{ mol L}^{-1}$  was 60.3%. The  $\text{IC}_{50}$  value was  $6.6 \times 10^{-5} \times 10^{-5} \text{ mol L}^{-1}$ . Hence, the HE–Eu(III) complex can be considered as a good scavenger of hydroxyl radicals.

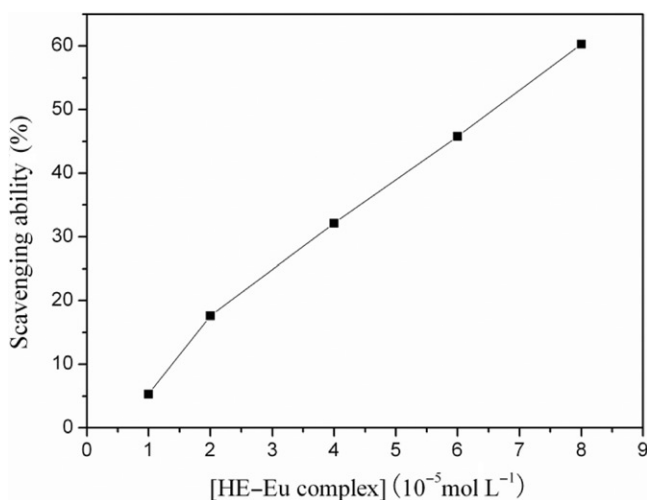


Figure 12. Hydroxy radical scavenging activity of HE-Eu(III) complex.

#### 4. Conclusion

Interaction between HE-Eu(III) complex and hsDNA has been studied in Tris-HCl buffer of pH=7.40 by spectral analysis and viscosity. The binding constants of HE-Eu(III) complex to DNA were  $K_{298\text{K}}^{\ominus} = 1.90 \times 10^5 \text{ L mol}^{-1}$  and  $K_{310\text{K}}^{\ominus} = 7.21 \times 10^5 \text{ L mol}^{-1}$  in an entropy-driven reaction. The present findings demonstrate that the interaction between HE-Eu(III) complex and hsDNA was partial intercalation binding and groove binding. The rigid plane of the complex partially intercalates into DNA base pairs, resulting in a kink in the DNA helix; because the phenolic hydroxyls of HE were prone to deprotonation, they could interact with the major or minor grooves of hsDNA through hydrogen bonds. The title complex was found to be a good scavenger of hydroxyl radicals. The results strongly support HE-Eu(III) complex having an important theoretical and practical value for the mechanism of drugs and drug design.

#### Acknowledgments

This study was supported by National Natural Science Foundation of China (no. 30572254) and Postgraduate Innovation Foundation of Southwest University of Science and Technology. We are grateful for the apparatus support of the Analytical and Testing Center of Southwest University of Science and Technology.

#### References

- [1] A. Erdem, M. Ozsoz. *Anal. Chim. Acta*, **437**, 107 (2001).
- [2] J.W. Kang, L. Zhuo, X.Q. Lu, H.D. Liu, M. Zhang, H.X. Wu. *J. Inorg. Biochem.*, **98**, 79 (2004).
- [3] F. Wang, Y.X. Xu, J. Zhao, S.S. Hu. *Bioelectrochemistry*, **70**, 356 (2007).

- [4] G.M. Zhang, Y.H. Pang, S.M. Shuang, C. Dong, M.M.F. Choi, D.S. Liu. *J. Photochem. Photobiol., A*, **169**, 153 (2005).
- [5] A. Radi, M.A.E. Ries, S. Kandil. *Anal. Chim. Acta*, **495**, 61 (2003).
- [6] N. Nizomov, E.N. Kurtaliev, S.N. Nizamov, G. Khodjayev. *J. Mol. Struct.*, **936**, 199 (2009).
- [7] G.W. Zhang, J.B. Guo, J.H. Pan, X.X. Chen, J.R. Wang. *J. Mol. Struct.*, **923**, 114 (2009).
- [8] M. Marinić, I. Piantanida, G. Rusak, M. Žinić. *J. Inorg. Biochem.*, **100**, 288 (2006).
- [9] H.R. Zare, N. Nasirizadeh. *Sensors Actuators, B*, **143**, 666 (2010).
- [10] L.S. Ren, J.G. Xu, J.Y. Ma. *Chin. J. Chin. Mater. Med.*, **15**, 50 (1990).
- [11] Y.B. Zhou, F.Z. Yao, J.R. Han, Y. Yang, C.F. Zhang, Y.P. Shi. *Chin. J. Integr. Trad. West. Med.*, **23**, 370 (2003).
- [12] N. Smirnoff, Q.J. Cumbes. *Phytochemistry*, **28**, 1057 (1989).
- [13] G. Barone, N. Gambino, A. Ruggirello, A. Silvestri, A. Terenzi, V.T. Liveri. *J. Inorg. Biochem.*, **103**, 731 (2009).
- [14] Z.H. Xu, F.J. Chen, P.X. Xi, X.H. Liu, Z.Z. Zeng. *J. Photochem. Photobiol., A*, **196**, 7783 (2008).
- [15] I.U.H. Bhat, S. Tabassum. *Spectrochim. Acta, Part A*, **72**, 1026 (2009).
- [16] G. Sathyaraj, T. Weyhermuller, B.U. Nair. *Eur. J. Med. Chem.*, **45**, 284 (2010).
- [17] A.A. Ouameur, R. Marty, H.A. Tajmir-Riahi. *Biopolymers*, **77**, 129 (2005).
- [18] Y. Wang, A.H. Zhou. *J. Photochem. Photobiol., A*, **190**, 121 (2007).
- [19] R. Vijayalakshmi, M. Kanthimathi, V. Subramanian. *Biochim. Biophys. Acta*, **1475**, 157 (2000).
- [20] S. Nafisi, A.A. Saboury, N. Keramat. *J. Mol. Struct.*, **827**, 35 (2007).
- [21] Y.T. Sun, S.Y. Bi, D.Q. Song, C.Y. Qiao, D. Mu, H. Zhang. *Sensors Actuators, B*, **129**, 799 (2008).
- [22] C.Q. Cai, X.M. Chen, F. Ge. *Spectrochim. Acta, Part A*, **76**, 202 (2010).
- [23] W.R. Ware. *J. Phys. Chem.*, **66**, 455 (1962).
- [24] J.P. Cheng, Q.Y. Lin, R.D. Hu, W.Z. Zhu, H.Q. Li, D.H. Wang. *Cent. Eur. J. Chem.*, **7**, 105 (2009).
- [25] J.B. Lepecq, C. Paoletti. *J. Mol. Biol.*, **27**, 87 (1967).
- [26] M.L. Guo, P. Yang, B.S. Yang, Z.G. Zhang. *Chin. Sci. Bull.*, **41**, 1098 (1996).
- [27] Z.G. Zhang, X.D. Dong. *Biomaterials*, **22**, 283 (2009).